RESEARCH ARTICLE

Lactococcus lactis D4 Restores Gut Microbiota Balance in Azoxymethane and Dextran Sulfate Sodium-induced Colorectal Cancer Rat Model

Rini Suswita[1,*], Muhammad Iqbal Rivai[1], Muhammad Iqbal[2], Irwan[1], Avit Suchitra[1]

[1]Department of Surgery, Faculty of Medicine, Universitas Andalas, Jl. Perintis Kemerdekaan No. 94, Padang, Indonesia
[2]Department of Anatomy, Faculty of Medicine, Universitas Andalas, Limau Manis, Pauh, Padang, Indonesia

*Corresponding author. Email: ristarini@gmail.com

Received date: Sep 6, 2024; Revised date: Nov 11, 2024; Accepted date: Nov 12, 2024

Abstract

BACKGROUND: Gut microbiota plays a crucial role in the initiation and progression of colorectal cancer (CRC), with various bacterial species including *Lactococcus lactis* implicated in this process. However, there is a lack of studies reporting the specific effects of *L. lactis* on microbiota balance in the context of CRC, especially strain D4. Therefore, this study was conducted to evaluate the effect of *L. lactis* D4 administration on gut microbiota balance in a rat model of CRC.

METHODS: This experimental study involved Sprague Dawley rats that were separated into untreated control (CO group), CRC-induced (CA group), and *L. lactis* D4-treated CRC-induced (LLD group). The CRC induction was performed by giving azoxymethane (AOM) and dextran sulfate sodium (DDS). Gut microbiota profile was analyzed using next generation sequencing (NGS), and microbial community dynamics were assessed through alpha and beta diversity metrics.

RESULTS: *L. lactis* D4 restored gut microbiota balance by regulating Firmicutes/Bacteroidota ratio, and changing the microbiota composition by increasing the number of bacteria from the phylum Actinobacteria and decreasing bacteria from the phylum Bacteroidota and Proteobacteria. Alpha diversity was reduced in the LLD group, suggesting a decreased bacterial diversity post-treatment, but more closely aligned with the CO group than the CA group. Beta diversity analysis showed that the microbial composition of the treated group was similar to the CO group, while the CA group exhibited a distinct microbiota profile, characterized by higher abundance of pathogenic bacteria and reducing beneficial microbial species.

CONCLUSION: *L. lactis* D4 administration effectively modulates gut microbiota in CRC model, enhancing the presence of beneficial bacteria from the Firmicutes and Bacteroidota phylum while suppressing pathogenic species from the Proteobacteria phylum.

KEYWORDS: colorectal cancer, gut microbiota, next generation sequencing, *Lactococcus lactis* D4

Indones Biomed J. 2024; 16(6): 517-26

Introduction

Colorectal cancer (CRC) is one of the most common cancers globally and a significant burden to public health. The incidence and mortality rates of CRC vary by region and are closely linked to socioeconomic factors. In recent years, there has been a concerning rise in CRC cases, particularly among younger populations, driven largely by changes in lifestyle and diet. This trend is especially notable in Asia, including Indonesia, where CRC ranks as the second most common cancer in men and the third in women.(1,2)

CRC is driven by a combination of genetic and environmental factors, with growing evidence highlighting the role of the gut microbiota in its development. Dysbiosis, or the imbalance of gut microbiota, has been implicated in the initiation, progression, and metastasis of CRC. Changes in microbial composition, especially the overgrowth of

pathogenic bacteria, are thought to contribute to the pro-inflammatory environment that fosters tumorigenesis.(3-8)

Recent studies underscore the significance of microbiota in cancer development, not just as a risk factor but also in the pathogenesis of autoimmune diseases. The gut microbiome plays a critical role in immune regulation, inflammation, and the integrity of the gut barriers, all of which are relevant to CRC pathogenesis. Notably, chronic inflammation, such as that seen in inflammatory bowel disease (IBD), promotes CRC development through the inflammation-dysplasia-carcinoma sequence.(10,11) The animal models using azoxymethane (AOM) and dextran sulfate sodium (DSS) have become standard for studying inflammation-related CRC. AOM induces mutations in colonic epithelial cells, while DSS disrupts the intestinal barrier, leading to inflammation and tumor formation. This model closely mimics the progression of CRC in humans, especially colitis-associated cancers.(12-20)

Probiotics have emerged as a promising strategy to restore gut microbiota balance and reduce inflammation. Probiotics are known to produce several bioactive molecules that act as antioxidants through various mechanisms, including the production of Exopolysaccharides (EPS) and superoxide dismutase (SOD).(21) *Lactococcus lactis* D4, isolated from the traditional Minangkabau fermented buffalo milk product dadih, has been shown to offer multiple health benefits. Recent research indicates that *L. lactis* D4 can modulate gut microbiota composition by increasing beneficial bacteria and suppressing pathogenic species associated with CRC. More importantly, *L. lactis* D4 has been shown to reduce chronic inflammation by suppressing the production of key pro-inflammatory cytokines, such as interleukin (IL)-6 and tumor necrosis factor (TNF)-α, which are major contributors to CRC progression.(22-25) *L. lactis* D4 may serve as a promising adjunct therapy for CRC prevention and management by restoring gut microbiota balance and reducing inflammation. Therefore, this study was conducted to investigate the effects of *L. lactis* D4 on modulating gut microbiota dysbiosis, a critical factor in the progression of CRC. Ultimately, *L. lactis* D4 might represent a potential therapeutic target in CRC management.

Methods

Study Design and Animal Model

This laboratory-based experimental study was conducted at Ina Lab Laboratory from May to October 2023, and utilized a randomized control group posttest-only design with Sprague Dawley rats aged 6-7 weeks and weighed 170-220 grams. A total of 42 male rats were involved in this research, and divided into research and evaluation groups. The research groups were then randomly separated into 3 different groups; the untreated control rats (CO group), which consisted of rats that were neither induced with cancer nor treated, serving as a baseline to represent the normal and healthy condition (n=10); the CRC-induced rats (CA group), which consisted of rats that were induced with CRC, but did not treated (n=10); and *L. lactis* D4-treated CRC-induced rats (LLD group), which consisted of rats that were induced with CRC, and later treated with *L. lactis* D4 (n=10). Two rats from the evaluation group (n=12) were terminated by cervical dislocation every two weeks for histopathological confirmation of CRC after the CRC-induction.

All rats were housed in standard laboratory conditions, with a 12-hour light/dark cycle and *ad libitum* access to food and water. The acclimatization period lasted for 1 week to ensure the animals adapted to the environment, followed by the CRC induction that began in week-2. The *L. lactis* D4 treatment was given after the CRC induction was ensured (Figure 1). Ethical guidelines for animal welfare were strictly followed throughout the study. The study protocol was approved by the Health Research Ethics Committee of the Faculty of Medicine, Universitas Andalas (Approval No.: 79/UN.162.KEP-FK/2023).

CRC Induction

The rats in CA, LLD, and the evaluation groups were induced with CRC by giving AOM (Cat No. A5486; Sigma-Aldrich, Saint Louis, MO, USA) injected intraperitoneally at a single dose of 10 mg/kgBW as well as 2.5% DSS (Cat No. 51227; Sigma-Aldrich) diluted in the rats' drinking water for 5 days. The induction process started on the first day of week-2. This induction procedure was repeated for three cycles.

Preparation and Administration of L. lactis D4

L. lactis D4 was isolated from 250 grams *Dadih* in bamboo tubes.(26) The bacteria were cultured using the streak quadrant method on MRS agar plates and incubated at 30°C for 48 hours. After incubation, the bacterial colonies were transferred to MRS broth and incubated at 30°C for 24 hours. Following this, the culture was centrifuged to separate the bacterial pellet, which was suspended to a final concentration of 1×10^9 CFU/mL. No additional dilution was required before administered to the rats.

L. lactis D4 was administered per rectal for 30 consecutive days to the rats in the LLD group after confirming

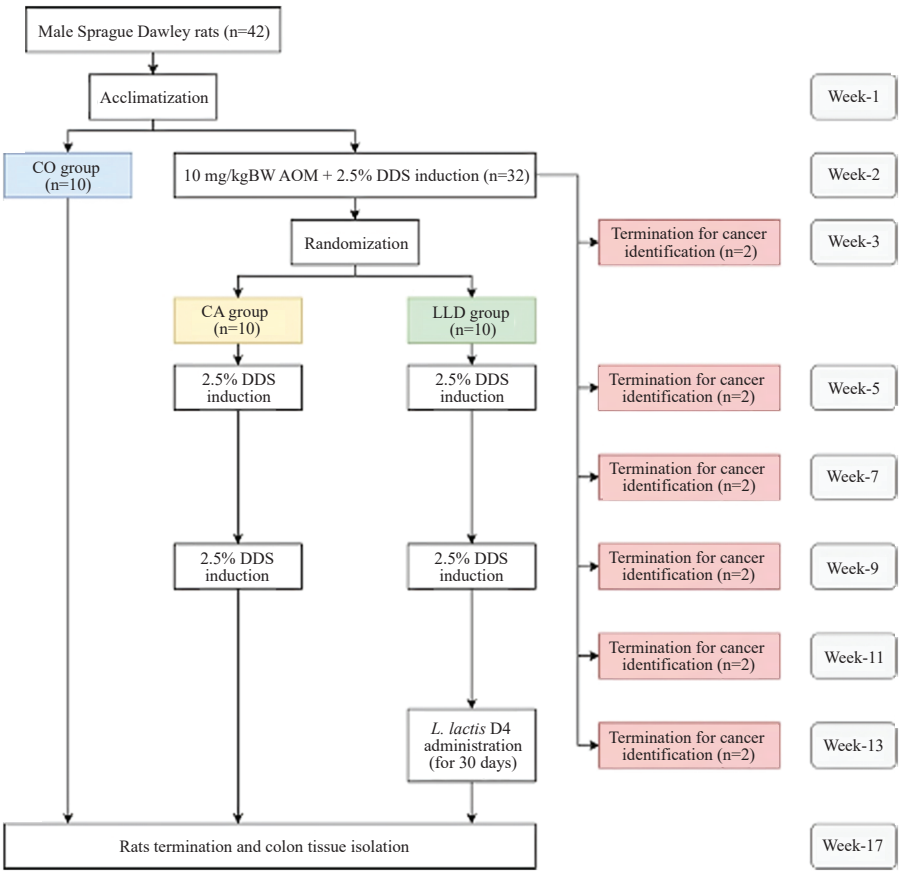

Figure 1. Study timeline and animal treatment procedure.

the presence of CRC in week-13. The dose of 1×10^9 CFU/mL in 0.5 mL was given daily. After the administration of *L. lactis* D4 in week-17, fecal samples were collected.

Microbiota Analysis and Sequencing

Fecal samples were collected from all groups at the end of the treatment period. Each sample (5 mg) underwent microbiota analysis using Next Generation Sequencing (NGS). The sequencing process involved DNA extraction, DNA shearing and quality control (QC), library preparation as well as sequencing and bioinformatics processing.

DNA extraction used a standard protocol optimized for microbial analysis employing the QIAamp Fast DNA Stool Mini Kit (Cat No. 51604; Qiagen, Hilden, Germany). The extracted DNA was then subjected to shearing using Long Light Tech equipment to ensure uniform fragment sizes. QC checks were performed on the DNA using the TurboCycler 2 Thermal Cycler (Blue-Ray Biotech, New Taipei City, Taiwan) to assessed the integrity and purity of the sheared DNA.

Library preparation and sequencing were carried out using Formulatrix automation equipment, and sequencing was performed on both the MGI Tech and Oxford Nanopore platforms. The 16S rRNA gene, specifically targeting the V3–V4 hypervariable regions, was amplified to analyze bacterial communities. Sequencing depth and coverage were adjusted to ensure accurate representation of microbial diversity.

Taxonomic assignment, from the phylum to the species level, was performed using the SILVA database (the 138 release) as the reference. The taxonomic ranks (phylum, class, order, family, genus, and species) were determined through alignment of the 16S rRNA sequences with known bacterial genomes in the database. For the presentation of the results, only the ten most abundant taxa at each taxonomic rank were included in the analysis to focus on the dominant bacterial groups and ensure clarity. Relative abundance data were calculated for each taxonomic level, providing insights into the bacterial composition across all samples.

Results

The rats in CA, LLD, and the evaluation groups were induced with AOM and DDS to create a CRC rat model. Histopathological analysis confirmed CRC development at week-13 in the evaluation group (Figure 2). In rats that were induced with CRC, moderate to severe dysplasia

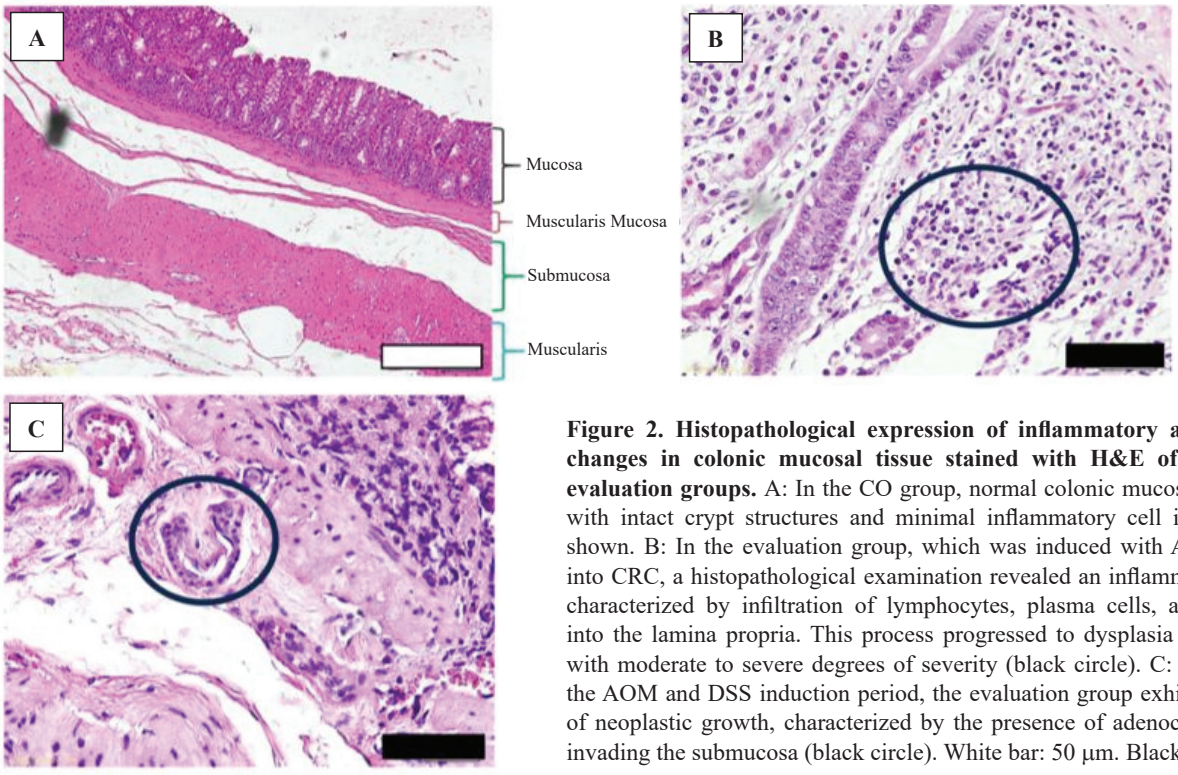

Figure 2. Histopathological expression of inflammatory and neoplastic changes in colonic mucosal tissue stained with H&E of the CO and evaluation groups. A: In the CO group, normal colonic mucosal architecture with intact crypt structures and minimal inflammatory cell infiltration was shown. B: In the evaluation group, which was induced with AOM and DSS into CRC, a histopathological examination revealed an inflammatory reaction characterized by infiltration of lymphocytes, plasma cells, and neutrophils into the lamina propria. This process progressed to dysplasia in colon cells, with moderate to severe degrees of severity (black circle). C: At week-13 of the AOM and DSS induction period, the evaluation group exhibited evidence of neoplastic growth, characterized by the presence of adenocarcinoma cells invading the submucosa (black circle). White bar: 50 µm. Black bar: 20 µm.

were observed compared to the CO group. There were also significant inflammatory and neoplastic changes, including dysplasia and abnormal glandular structures, indicating a pronounced pathological response.

Sequencing Results and Data Processing

The sequencing results include raw paired-end (RawPE) sequences, which were processed to identify valid sequence reads. A total of 183,258 sequence reads were obtained for the LLD group, 103,079 for the CA group, and 174,420 for the CO group, as shown in the Nochime (Table 1). These processed sequences formed the basis for further analyses of microbial composition.

Operational Taxonomic Unit (OTU)/Amplicon Sequence Variant (ASV) Analysis

The OTU/ASV analysis revealed distinct bacterial populations across the groups. OTUs were used for grouping bacterial sequences with 97% similarity, while ASVs were employed to identify unique sequences. Both methods demonstrated changes in microbial composition across the research groups, further detailed in the following sections.

Relative Abundance in Phylum Level

The relative abundance analysis identified the top 10 most abundant bacterial phyla across the different groups. Firmicutes exhibited the highest relative abundance in all groups, followed by Actinobacteria, Bacteroidota, and Proteobacteria (Figure 3A). In the CO group, Firmicutes was the most dominant phylum (mean = 101,968.70), whereas the CA group exhibited a significantly higher presence of Bacteroidota (mean = 15,215.60), indicating gut dysbiosis associated with CRC. Notably, after treatment with *L. lactis* D4, the LLD group demonstrated a shift back toward Firmicutes dominance (mean = 114,289.80), suggesting that *L. lactis* D4 restored microbial balance (Table 2). The Kruskal-Wallis test revealed significant differences in bacterial abundance at the phylum level between groups

Table 1. Processing data of sequencing results.

Group	RawPE	Combined	Qualified	Nochime	Base(nt)	Avglen(nt)	GC	Q20	Q30	Effective Percentage
LLD	2,050,092	200,022	194,959	183,258	77,383,221	42,226	52.91%	98.10%	94.01%	89.35%
CA	118,111	115,534	113,169	103,079	42,942,471	41,660	53.37%	98.27%	94.39%	87.27%
CO	202,161	197,695	193,197	174,420	73,216,339	41,977	53.79%	98.18%	94.26%	86.28%

(p<0.001). Interestingly, the values of Firmicutes in the LLD group were nearly identical to those in the CO group, reflecting that the treatment with *L. lactis* D4 reestablished a microbial state similar to the healthy condition.

Relative Abundance in Class Level

Further analysis was conducted at the class level to explore the dynamics within the Firmicutes phylum, highlighting the predominance of Bacilli, Clostridia, and Negativicutes. The CO group displayed a high abundance of Bacilli, consistent with its healthy gut profile, while the CA group showed a decrease in Bacilli and an increase in Clostridia, associated with CRC progression. After treatment, the LLD group showed a significant recovery in Bacilli levels and a decrease in Clostridia, reflecting a return to a healthier state similar to the CO group (Figure 3B). The consistent abundance values of Bacilli between the LLD and CO groups suggest that *L. lactis* D4 effectively restores the gut microbiota to a state that resembles a healthy microbiome. The Kruskal-Wallis test confirmed significant differences at the class level (p<0.001) (Table 3).

While Bacilli and its orders showed positive modulation, other classes like Negativicutes, Gammaproteobacteria, and Bacteroidia also presented interesting findings. Their increased presence in the CA group suggests a response to the dysbiotic and inflammatory environment of CRC. Negativicutes are typically beneficial but may rise in response to inflammation, reflecting an adaptive reaction rather than an indication of health. Gammaproteobacteria thrive in stressed conditions, and their elevated levels in CRC conditions suggest adaptability to inflammation and tumor microenvironments. Bacteroidia, known for their short-chain fatty acid (SCFA) production, may increase as a compensatory response to dysbiosis but have limited anti-inflammatory impact in the inflamed CRC environment.

Relative Abundance in Order Level

At the order level, the uneven abundance of bacteria among samples becomes apparent, with some samples showing significantly higher abundance of a certain order compared to others (Figure 3C). Analyzing the Bacilli class at the order level, Lactobacillales was the most dominant order in the LLD group, surpassing its abundance in the CA group, which had diminished due to dysbiosis (Figure 3C). The increase in Lactobacillales in the LLD group emphasizes the beneficial modulation by *L. lactis* D4, promoting the recovery of gut health. The CO group had a higher proportion of Staphylococcales, which is associated with certain pathogenic traits and was reduced in the CA group during colitis-associated cancer (CAC). Microbes mostly work by CAC mechanism.

Relative Abundance in Family-Genus-Species Level

The family-genus-species level further details the abundance of bacteria, which show variety of bacteria abundance in the CO, CA, and LDD groups (Figure 3E, 3F, and 3G). Further analysis at the family-genus-species level revealed that *Lactobacillaceae* (family) and *Lactobacillus* (genus) were significantly more abundant in the LLD group, corroborating the restored *Firmicutes* dominance (Figure 3E and 3F). This detailed examination demonstrates that the increase in beneficial *Lactobacillales* and associated genera contributes to the recovery of the gut microbiota, enhancing microbial health and potentially mitigating CRC progression. The consistent restoration of these beneficial orders and families in the LLD group to levels resembling the CO group supports the idea that *L. lactis* D4 fosters a healthy microbial environment and reduces pathogenic bacterial influence.

Alpha and Beta Diversity

Table 4 presented alpha diversity metrics, including the Simpson diversity index, which quantifies microbial diversity within each group. The LLD group had a Simpson index of 0.94, indicating lower diversity compared to CO (0.94) and CA (0.98) groups. The reduction in microbial diversity following *L. lactis* D4 treatment in the LLD group suggests a shift toward a more specialized bacterial community, reflecting a positive restoration of gut microbiota balance.

Figure 3D illustrated the beta diversity using the Unweighted Pair-group Method with Arithmetic Mean (UPGMA) analysis, which visualizes the similarities between bacterial compositions in the three groups. The LLD group showed greater similarity to the CO group, indicating that the administration of *L. lactis* D4 reduced dysbiosis. In contrast, the CA group exhibited a distinct microbial profile, confirming cancer-associated dysbiosis. These findings highlight the effectiveness of *L. lactis* D4 in restoring microbiota composition in the LLD group. These dissimilarity coefficient between any pair of CO, CA, and LLD groups were shown in Figure 4. The weighted UniFrac distance accounts for both the presence and abundance of microbial taxa, while the unweighted UniFrac distance only considers the presence or absence of taxa. A higher beta diversity coefficient indicates a greater difference in microbial communities between the groups. For example, the dissimilarity between the CA and LLD groups shows a

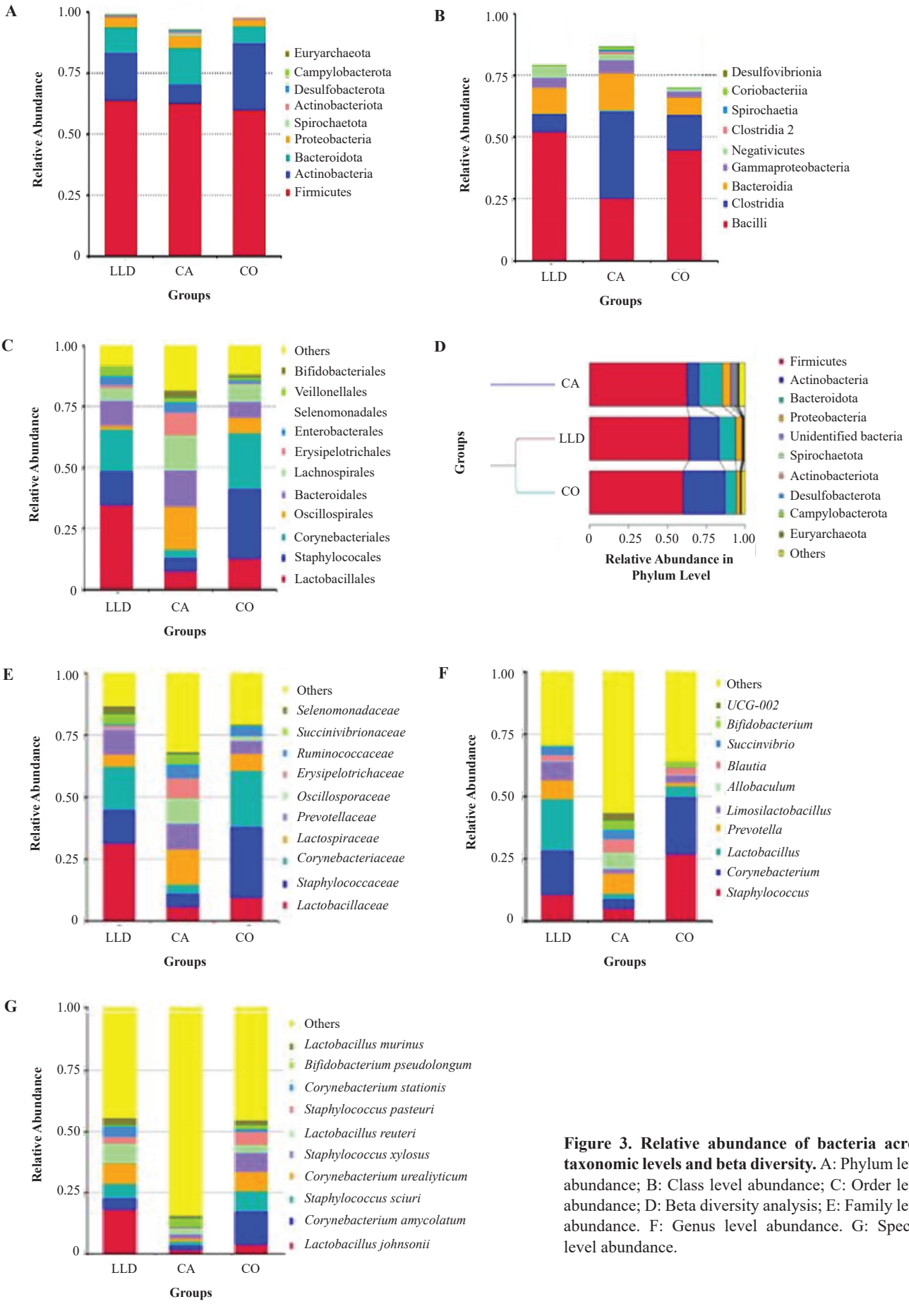

Figure 3. Relative abundance of bacteria across taxonomic levels and beta diversity. A: Phylum level abundance; B: Class level abundance; C: Order level abundance; D: Beta diversity analysis; E: Family level abundance. F: Genus level abundance. G: Species level abundance.

Table 2. Mean differences bacterial abundance at phylum level.

Colon Microbiota	Mean±SD			*p*-value
	LLD Group (n=10)	CA Group (n=10)	CO Group (n=10)	
Firmicutes	114,289.80±7,650.69	62,637.30±5,090.43	101,968.70±7,370.92	<0.001*[a]
Actinobacteria	34,416.50±3,441.84	7,290.30±235.79	4,095.50±64.87	<0.001*[b]
Bacteroidota	19,268.00±959.94	15,215.60±1,068.46	11,211.80±735.40	<0.001*[a]
Proteobacteria	7,389.90±318.03	5,201.50±231.48	5,672.00±247.11	<0.001*[b]
Spirochaetota	18,040.00±13.90	92,530.00±90.43	314.50±23.60	<0.001*[b]
Actinobacteriota	58,710.00±25.54	81,150.00±31.32	76,050.00±24.78	<0.001*[b]
Desulfobacterota	55,800.00± 63.00	81,780.00±51.42	11,510.00±9.52	<0.001*[a]
Campylobacterota	14,590.00±16.39	27,210.00±18.57	43.80±2.53	<0.001*[a]
Euryarchaeota	20.00±1.56	247.80±24.31	153.50±3.03	<0.001*[a]

*Significant if $p<0.05$, [a]analyzed with One-way ANOVA, [b]analyzed with Kruskal-Wallis.

weighted UniFrac value of 0.448 and an unweighted value of 0.335, indicating significant differences in microbial composition, particularly when accounting for relative abundances. In contrast, the CO group shows no significant difference (0.0), suggesting similar microbial compositions across control samples.

Statistical Significance and Effect Sizes

The results showed statistically significant differences in bacterial abundance and diversity across all taxonomic levels ($p<0.001$). The effect sizes for each outcome, especially phylum and class were presented in Table 2 and Table 3, demonstrating the magnitude of differences between groups. The largest effect sizes were observed for changes in the Firmicutes and Bacteroidota phylum, as well as Bacilli and Clostridia classes, particularly between the CA and LLD groups, reinforcing the positive impact of *L. lactis* D4 on gut microbiota. These visual representations clearly demonstrate the reduction in dysbiosis markers and the significant improvement in microbial balance following *L. lactis* D4 treatment.

Discussion

The data processing steps outlined in Table 1 elucidate the transformation from RawPE sequences to the final Nochime sequences used for subsequent analyses. The reduction in sequence count from RawPE to Nochime indicates the elimination of sequences during processing, emphasizing the importance of quality control.(27) Parameters such as GC content, Q20, and Q30 provide crucial information about the quality and reliability of the obtained sequences.(28) The final valid sequences for analysis were 183.25 for LLD group, 103.08 for CA group, and 174.42 for CO group.

The insights gained from the NGS amplicon metagenomic sequencing shed light on the microbial diversity, especially when comparing samples from LLD, CA, and CO groups. The analysis of relative abundance, alpha diversity, and beta diversity patterns among these samples reveals distinct microbiota dynamics. The successful merging and sequencing quality, including parameters like

Table 3. Mean differences bacterial abundance at class level.

Colon Microbiota	Mean±SD			*p*-value
	LLD Group (n=10)	CA Group (n=10)	CO Group (n=10)	
Bacilli	94,608.00±4,059.34	25,006.50±3,969.22	76,526.40±1,960.28	<0.001*[a]
Clostridia	12,828.80±696.06	34,205.10±2,581.44	24,961.30±2,732.08	<0.001*[a]
Bacteroidia	19,182.50±724.78	15,771.50±2,228.58	11,307.80±700.80	<0.001*[a]
Gammaproteobacteria	7,438.90±317.25	5,180.20±154.68	4,256.10±142.20	<0.001*[a]
Negativicutes	8,354.60±263.30	2,302.20±259.70	1,613.80±309.90	<0.001*[b]
Clostridia 2	382.00±13.50	1,282.60±135.90	290.80±46.50	<0.001*[a]
Spirochaetia	182.60±16.50	923.40±122.90	301.70±34.70	<0.001*[b]
Coriobacteriia	596.00±96.50	811.90±74.80	770.40±62.20	<0.001*[a]
Desulfovibrionia	523.10±49.40	807.90±70.80	107.50±14.06	<0.001*[a]

*Significant if $p<0.05$, [a]analyzed with One-way ANOVA, [b]analyzed with Kruskal-Wallis.

Table 4. Alpha diversity.

Group	Observed Species	Shannon	Simpson	Chao1	ACE	Goods Coverage	PD Whole Tree
LLD	465	5.08	0.94	570.21	558.10	1.00	38.76
CA	675	6.96	0.98	675.87	677.86	1.00	52.19
CO	598	5.58	0.95	656.10	650.19	1.00	47.95

GC content, Q20, and Q30, are vital for understanding the reliability and accuracy of the obtained data. Comparing these samples provides valuable information on microbial diversity differences, offering insights into microbial composition and potential ecological interactions within the samples.(29-31)

Furthermore, the implications of these findings in a research context are substantial. The data from NGS amplicon metagenomic sequencing can guide further research directions, including investigating the functional potential of the microbiota, exploring microbial interactions, and understanding microbiota dynamics in response to environmental changes. The findings also pave the way for longitudinal studies to assess temporal dynamics of microbial diversity and intervention studies to elucidate the impact of specific environmental factors on microbiota composition and function.(32,33)

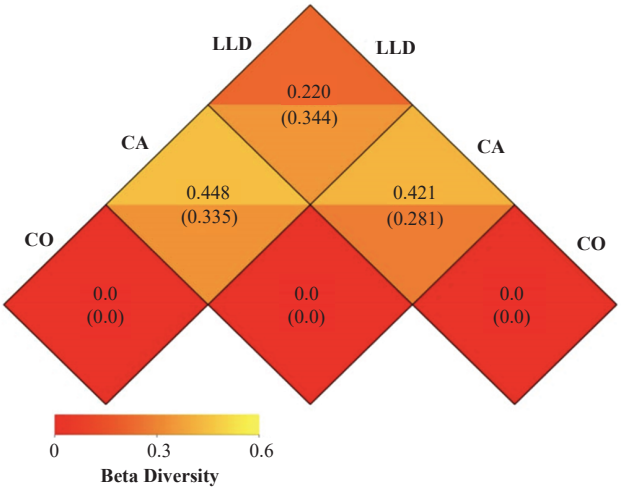

Figure 4. Beta diversity heatmap, which each grid represents dissimilarity coefficient between pairwise samples. Color differences indicate how similar or different of taxonomic diversity among these groups based on Weighted UniFrac distance value (above) and Unweighted UniFrac distance value (below). The Weighted UniFrac distance gives comparatively more importance to abundant lineages, while the Unweighted UniFrac distance gives more importance to rare lineages. The highest beta diversity value in Weighted UniFrac results was 0.448 between LLD and CA groups, whereas the lowest value was 0.220 between LLD group itself. Unweighted UniFrac results showed the highest value (0.344) was in LLD group, whereas the lowest value (0.281) between CA and LLD groups. The smaller the discrepancy coefficient between two groups, the smaller the difference in species diversity and *vice versa*.

The analysis of sequencing results involved the detection of numerous sequences from environmental samples, originating from bacteria in the studied environment. OTU and ASV analyses were crucial for characterizing taxonomic profiles and enhancing data interpretation. The taxonomic annotation obtained from OTU or ASV provides essential information about bacterial taxonomy, aiding in the display of Relative Abundance more interactively.(33) OTU and ASV play pivotal roles in annotating the taxonomy of obtained bacterial sequences. The taxonomic annotation offers insights into the taxonomy of bacteria at various levels, facilitating the efficient analysis of relative bacterial abundance. The use of NGS technology, particularly OTU and ASV analyses, has significantly advanced microbial ecology research. These approaches contribute to unraveling taxonomic composition and community diversity, enhancing the interpretation of sequencing data.(34)

Practical implications of employing OTU and ASV in microbial ecology research are significant. These methods allow researchers to assess microbial diversity, community dynamics, and ecological interactions at high resolution, improving our understanding of microbial ecosystems.(34) However, challenges such as bacterial contamination in NGS datasets and variability in taxonomic annotation across different sequencing regions need addressing to ensure the accuracy and reliability of microbial diversity assessments. The choice between OTU and ASV methodologies is crucial, considering the trade-offs between sensitivity and specificity in microbial diversity analysis.(35)

However, the rat model for CRC used in this study might not fully replicate the complexities of human CRC. While the findings suggest that *L. lactis* D4 modulates gut microbiota and may offer therapeutic benefits, the applicability of these results to human cases of CRC remains uncertain. Further studies are required to determine whether these effects can be translated to human clinical settings, and should explore the feasibility of clinical trials in humans, focusing on safety, optimal dosing, and long-term effects of *L. lactis* D4 in CRC prevention and treatment.

Conclusion

This study demonstrated that *L. lactis* D4 treatment significantly altered gut microbiota composition, increasing sequence reads and reducing dysbiosis in a CRC model. The group of CRC-induced rats that were treated with *L. lactis* D4 showed a microbiota profile more similar to untreated rats than CRC-induced rats, with Firmicutes as the dominant phylum and Bacilli most prevalent at the class level. These findings suggest that *L. lactis* D4 restores gut microbiota balance and decreases colorectal tumorigenesis in colitis-associated CRC.

Authors Contribution

All authors made significant contributions to the conceptualization, data curation, funding acquisition, investigation, and methodology of the study. RS, MI, MIR, AS, and IR were involved in the project administration, resource allocation, supervision, and validation of the research. The visualization of the results was carried out by RS, MI, MIR, AS, and IR. All authors, including RS, MI, MIR, AS, and IR, contributed to the original draft writing and participated in the review and editing process to finalize the manuscript for submission.

References

1. Hossain MS, Karuniawati H, Jairoun AA, Urbi Z, Ooi J, John A, *et al.* Colorectal cancer: A review of carcinogenesis, global epidemiology, current challenges, risk factors, preventive and treatment strategies. Cancers. 2022; 14(7): 1732. doi: 10.3390/cancers14071732.
2. Faroque H, Aria NS, Muzilah NA, Al-Jamal HAN, Rahim MFA, Nakamura Y, *et al.* CHEK1 and GFPT1 as potential blood-based biomarkers for colorectal cancer. Indones Biomed J. 2023; 15(6): 358-65.
3. Movsisyan AS, Maguire FB, Parikh-Patel A, Gholami S, Keegan THM. Increasing rates of colorectal cancer among young people in California, 1988-2017. J Registry Manag. 2021; 48(4): 152-60.
4. Vallis J, Wang PP. Chapter 2: The role of diet and lifestyle in colorectal cancer incidence and survival. In: Morgado-Diaz JA, editor. Gastrointestinal cancers. Brisbane: Exon Publications; 2022.
5. Purnomo HD, Permatadewi CO, Prasetyo A, Indiarso D, Hutami HT, Puspasari D, *et al.* Colorectal cancer screening in Semarang, Indonesia: A multicenter primary health care based study. PLoS One. 2023; 18(1): e0279570. doi: 10.1371/journal.pone.0279570.
6. Luminthurahardjo W, Soeatmadji DW, Mintaroem K, Rahajoe P, Sandra F. N-Cadherin as an important marker in colorectal cancer: An investigation of β-catenin and cadherin expressions of SW-480 and HCT-116 cell lines. Indones Biomed J. 2021; 13(3): 289-94.
7. Porter RJ, Arends MJ, Churchhouse AMD, Din S. Inflammatory bowel disease-associated colorectal cancer: Translational risks from mechanisms to medicines. J Crohns Colitis. 2021; 15(12): 2131-41.
8. Lucafò M, Curci D, Franzin M, Decorti G, Stocco G. Inflammatory bowel disease and risk of colorectal cancer: An overview from pathophysiology to pharmacological prevention. Front Pharmacol. 2021; 12: 772101. doi: 10.3389/fphar.2021.772101.
9. Nardone OM, Zammarchi I, Santacroce G, Ghosh S, Iacucci M. Inflammation-driven colorectal cancer associated with colitis: From pathogenesis to changing therapy. Cancers. 2023; 15(8): 2389. doi: 10.3390/cancers15082389.
10. Tanaka T, Kohno H, Suzuki R, Yamada Y, Sugie S, Mori H. A novel inflammation-related mouse colon carcinogenesis model induced by azoxymethane and dextran sodium sulfate. Cancer Sci. 2003; 94(11): 965-73.
11. Tian R, Zuo X, Jaoude J, Mao F, Colby J, Shureiqi I. ALOX15 as a suppressor of inflammation and cancer: Lost in the link. Prostaglandins Other Lipid Mediat. 2017; 132: 77-83.
12. Ohnishi S, Hiramoto K, Ma N, Kawanishi S. Chemoprevention by aspirin against inflammation-related colorectal cancer in mice. J Clin Biochem Nutr. 2021; 69(3): 265-71.
13. Yang X, Wang Q, Zhang X, Li L, Cao X, Zhou L, *et al.* Purple yam polyphenol extracts exert anticolitis and anticolitis-associated colorectal cancer effects through inactivation of NF-κB/p65 and STAT3 signaling pathways. J Agric Food Chem. 2023; 71(32): 12177-89.
14. Stolfi C, Rizzo A, Franzè E, Rotondi A, Fantini MC, Sarra M, *et al.* Involvement of interleukin-21 in the regulation of colitis-associated colon cancer. J Exp Med. 2011; 208(11): 2279-90.
15. Zhang B, Xu Y, Liu S, Lv H, Hu Y, Wang Y, *et al.* Dietary supplementation of foxtail millet ameliorates colitis-associated colorectal cancer in mice via activation of gut receptors and suppression of the STAT3 pathway. Nutrients. 2020; 12(8): 2367. doi: 10.3390/nu12082367.
16. Ock CY, Kim EH, Hong H, Hong KS, Han YM, Choi KS, *et al.* Prevention of colitis-associated colorectal cancer with 8-hydroxydeoxyguanosine. Cancer Prev Res. 2011; 4(9): 1507-21.
17. Meana C, García-Rostán G, Peña L, Lordén G, Cubero Á, Orduña A, *et al.* The phosphatidic acid phosphatase lipin-1 facilitates inflammation-driven colon carcinogenesis. JCI Insight. 2018; 3(18): e97506. doi:10.1172/jci.insight.97506.
18. Saadatdoust Z, Pandurangan AK, Ananda Sadagopan SK, Mohd Esa N, Ismail A, Mustafa MR. Dietary cocoa inhibits colitis associated cancer: a crucial involvement of the IL-6/STAT3 pathway. J Nutr Biochem. 2015; 26(12): 1547-58.
19. Khalyfa AA, Punatar S, Aslam R, Yarbrough A. Exploring the inflammatory pathogenesis of colorectal cancer. Diseases. 2021; 9(4): 79. doi: 10.3390/diseases9040079.
20. Meiliana A, Wijaya A. Gut microbiota, obesity and metabolic dysfunction. Indones Biomed J. 2011; 3(3): 150-67.
21. Valentina I, Achadiyani, Adi SS, Lesmana R, Farenia R. Effect of Lactococcus reuteri administration on wrinkle formation and type I procollagen levels in UVB-exposed male Balb/c mice (Mus musculus). Mol Cell Biomed Sci. 2020; 4(3): 113-20.
22. Rosenberg E, DeLong EF, Thompson F, Lory S, Stackebrandt E. The Prokaryotes: Human Microbiology. 4th ed. New York: Springer; 2013.
23. Cheng Y, Ling Z, Li L. The intestinal microbiota and colorectal cancer. Front Immunol. 2020; 11: 615056. doi: 10.3389/fimmu.2020.615056.
24. Suswita R, Alvarino A, Darwin E, Jamsari J. Lactococcus lactis D4 has potential effect to alleviate inflammation and reverse dysbiosis in colitis rat model. Indones Biomed J. 2024; 16(2): 199-206.

25. Yu D, Xia Y, Ge L, Tan B, Chen S. Effects of Lactococcus lactis on the Intestinal Functions in Weaning Piglets. Front Nutr. 2021; 8: 713256. doi:10.3389/fnut.2021.713256.
26. Sukma A. Analysis of Microbiota in, and Isolation of Nisin-producing Lactococcus lactis subsp. lactis Strains from Indonesian Traditional Fermented Milk, Dadiah [Dissertation]. Okayama: Okayama University; 2017.
27. DNA qualification workflow for next generation sequencing of histopathological samples. PLoS One. 2013; 8(6): e62692. doi: 10.1371/journal.pone.0062692.
28. Jovel J, Patterson J, Wang W, Hotte N, O'Keefe S, Mitchel T, *et al.* Characterization of the gut microbiome using 16S or shotgun metagenomics. Front Microbiol. 2016; 7: 459. doi: 10.3389/fmicb.2016.00459.
29. Poretsky R, Rodriguez-R LM, Luo C, Tsementzi D, Konstantinidis KT. Strengths and limitations of 16S rRNA gene amplicon sequencing in revealing temporal microbial community dynamics. PLoS One. 2014; 9(4): e93827. doi:10.1371/journal.pone.0093827.
30. Rezasoltani S, Ahmadi Bashirzadeh D, Nazemalhosseini Mojarad E, Asadzadeh Aghdaei H, Norouzinia M, Shahrokh S. Signature of gut microbiome by conventional and advanced analysis techniques: Advantages and disadvantages. Middle East J Dig Dis. 2020; 12(1): 5-11.
31. Zheng X, Zhu Q, Qin M, Zhou Z, Liu C, Wang L, *et al.* The role of feeding characteristics in shaping gut microbiota composition and function of Ensifera (Orthoptera). Insects. 2022; 13(8): 719. doi: 10.3390/insects13080719.
32. Sharpton TJ. An introduction to the analysis of shotgun metagenomic data. Front Plant Sci. 2014; 5: 209. doi: 10.3389/fpls.2014.00209.
33. Chiarello M, McCauley M, Villéger S, Jackson CR. Ranking the biases: The choice of OTUs vs. ASVs in 16S rRNA amplicon data analysis has stronger effects on diversity measures than rarefaction and OTU identity threshold. PLoS One. 2022; 17(2): e0264443. doi: 10.1371/journal.pone.0264443.
34. Shah N, Meisel JS, Pop M. Embracing ambiguity in the taxonomic classification of microbiome sequencing data. Front Genet. 2019; 10: 1022. doi: 10.3389/fgene.2019.01022.
35. Human Microbiome Project Consortium. A framework for human microbiome research. Nature. 2012; 486(7402): 215-21.